2-1-2021

Impact of bandwidth on antenna-array noise matching

Roshaan Ali
University of Calgary

Leonid Belostotski
University of Calgary

Geoffrey G. Messier
University of Calgary

Arjuna Madanayake
Florida International University

Adrian T. Sutinjo
Curtin University

Impact of bandwidth on antenna-array noise matching

Roshaan Ali,[1] Leonid Belostotski,[1,✉] Geoffrey G. Messier,[1] Arjuna Madanayake,[2] and Adrian T. Sutinjo[3]

[1] Department of Electrical and Computer Engineering, The University of Calgary, 2500 University Drive, Calgary, Alberta, T2N1N4, Canada (E-mail: alir@ucalgary.ca, gmessier@ucalgary.ca)

[2] Department of Electrical and Computer Engineering, Florida International University, 10555 West Flagler Street, Miami, Florida, 33174, USA (E-mail: amadanay@fiu.edu)

[3] International Centre for Radio Astronomy Research, Curtin Institute of Radio Astronomy, Curtin University, 1 Turner Ave, Bentley, WA, 6102, Australia (E-mail: adrian.sutinjo@curtin.edu.au)

✉E-mail: lbelosto@ucalgary.ca

This letter expands the treatments of wideband noise analysis of antenna arrays by including bandwidth effects on beam-equivalent receiver noise temperature, T_{rec}, and the active reflection coefficient, Γ_{act}. The particular focus of the letter is on receiver noise decorrelation in wideband systems having noise bandwidth $f_{\mathrm{B}} \gg 1$ Hz. The new analysis and simulations show increase in T_{rec} and the departure of Γ_{act} from that obtained using contemporary analyses for $f_{\mathrm{B}} = 1$ Hz. Although the paper also shows that for many applications over moderate bandwidths and close connection between the receiver and array the influence of f_{B} on T_{rec} is not significant, the simulations of a 71-element array demonstrate that the noise decorrelation due to wide f_{B} can result in tens of percent (as much as 45.5% in simulations described in this letter) increase in T_{rec} above the low-noise amplifier minimum noise temperature, which should be taken into account at the design stage of ultra-wide band systems, such as those under investigation by, for example, the Defense Advanced Research Project Agency (DARPA) in its wideband adaptive RF protection (WARP) program and ultra-sensitive active electronically scanned array (AESA) radars for tracking stealth objects.

Introduction: Antenna arrays see ever-expanding application in communications (e.g. emerging 5G and 6G systems, massive, and holographic MIMO systems), radar, radio astronomy, magnetic resonance imaging, remote sensing, signal intelligence, and spectrum sensing [1–11]. Past research showed that minimizing the noise of a receiving antenna array requires the optimum reflection coefficient for minimum noise, $\Gamma_{\mathrm{opt}} \in \mathbb{C}$, of the receiver front-end low-noise amplifier (LNA) to equal the 'active' reflection coefficient, $\Gamma_{\mathrm{act}} \in \mathbb{C}$, of the antenna array [12–16]. The determination of Γ_{act} requires the knowledge of beamforming coefficients and the electrical parameters, for example, S-parameters, of the antenna array. However, typically focusing on narrow-band applications, prior analyses did not consider the effects of noise bandwidth on Γ_{act}. As such, a typical noise analysis was performed at a single frequency for a 1-Hz bandwidth and simply extended to wideband by multiplying the resultant noise power by the desired bandwidth.

For each frequency of array operation, the conventional noise analysis proceeds as follows: (a) S-parameters of an antenna array and the LNA are simulated or measured in a 1-Hz bandwidth, f_{B0}; (b) noise parameters (NPs) of the LNA are simulated in a 1-Hz bandwidth or measured over a ~1-MHz bandwidth, $f_{\mathrm{B,np}}$, and the NPs are assumed to be invariant of $f_{\mathrm{B,np}}$; (c) noise power at the array output, beam-equivalent receiver noise temperature, T_{rec}, and Γ_{act} are calculated in a 1-Hz bandwidth based on the results in (a) and (b) and the knowledge of the beamformer coefficients [12, 14–16]; and, if needed, (d) T_{rec} and Γ_{act} are assumed unchanged over operating noise bandwidth f_{B}, and the output noise power for f_{B} is calculated by multiplying the result in (c) by f_{B}.

Three observations are made: (a) measured S-parameters manifest any propagation delays through the array as phases at each frequency; (b) while wide $f_{\mathrm{B,np}}$ increases the LNA output noise power and accelerates measurements, the assumption of LNA NP invariance on $f_{\mathrm{B,np}}$ is not accurate as it ignores bandwidth-dependent decorrelation of LNA noise sources [17]; and (c) the linear scaling of the output noise power by f_{B} may also be inaccurate due to noise decorrelation problem akin discussions in [17]. This last observation has not been investigated in the past for compact arrays, while for physically large antenna arrays, such as single-pixel aperture-synthesis radio telescopes, it is well known that even bandwidths of a few kHz result in noise decorrelation [18]. Therefore, this work investigates f_{B} impact of noise decorrelation on T_{rec} and Γ_{act} of wideband compact arrays. Note that as f_{B} is the noise bandwidth, it may be much narrower than the RF system bandwidth; therefore, in this work "wideband" refers to wide noise bandwidths.

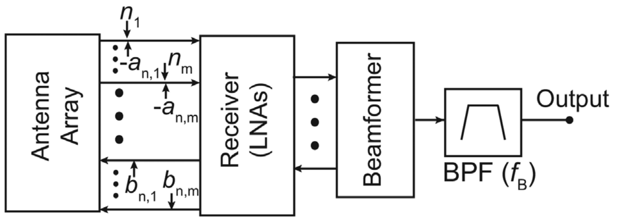

Fig. 1 *Block diagram of the network*

T_{rec} and Γ_{act} dependence on bandwidth: As already stated above, prior works analyzed array noise temperatures in a 1-Hz bandwidth. While 1-Hz bandwidth is conventional, in practice most array receivers operate with $f_{\mathrm{B}} \gg 1$ Hz. To investigate the impact of f_B on T_{rec} and Γ_{act}, we start by considering an m-element array representation in Figure 1. The formulations from (31) of [15] describes T_{rec} as

$$T_{\mathrm{rec}} = T_0 \frac{\mathbf{w}^{\dagger}\mathbf{G}\mathbf{R}_{\mathrm{rec}}\mathbf{G}^{\dagger}\mathbf{w}}{\mathbf{w}^{\dagger}\mathbf{G}\mathbf{R}_{\mathrm{t}}\mathbf{G}^{\dagger}\mathbf{w}}, \tag{1}$$

where $(\cdot)^{\dagger}$ denotes Hermitian conjugate, $T_0 = 290$ K is the reference temperature, $\mathbf{w} \in \mathbb{C}^m$ is the vector of m beamformer coefficients,

$$\mathbf{G} = \sqrt{R_0}\,(\mathbf{I} + \mathbf{S}_A)\,(\mathbf{I} - \mathbf{S}_R\mathbf{S}_A)^{-1} \tag{2}$$

relates the forward waves of the noise emanating from the array ports to the receiver output, $\mathbf{S}_R \in \mathbb{C}^{m\times m}$ is a matrix of receiver reflection coefficients, $R_0 \in \mathbb{R}$ is the characteristic impedance, $\mathbf{I}$ is the identify matrix, $\mathbf{R}_{\mathrm{rec}} \in \mathbb{C}^{m\times m}$ is the receiver noise correlation matrix, and $\mathbf{R}_{\mathrm{t}} \in \mathbb{C}^{m\times m}$ is the array noise correlation matrix. White-thermal-noise waves, which are identified by a vector $\mathbf{n} = [n_1 \ldots n_{\mathrm{m}}]$ in Figure 1 and emanate from the ports of each element of the array, are uncorrelated [19]. On the other hand, the corresponding terms of the two noise wave vectors $\mathbf{a}_{\mathrm{n}} = [a_{\mathrm{n},1} \ldots a_{\mathrm{n,m}}]$ and $\mathbf{b}_{\mathrm{n}} = [b_{\mathrm{n},1} \ldots b_{\mathrm{n,m}}]$ that are emanating from each LNA are correlated. This correlation is advantageous and is used for minimizing the receiver noise by appropriately scaling and phasing $\mathbf{b}_{\mathrm{n}}$ so that when combined with $\mathbf{a}_{\mathrm{n}}$ in the receiver their correlated portion destructively interfered [20]. This minimization is accomplished by reflecting $\mathbf{b}_{\mathrm{n}}$ either off an antenna with a reflection coefficient $\Gamma_{\mathrm{s}} = \Gamma_{\mathrm{opt}}$ in a single-antenna system or off an effective reflection coefficient, known as Γ_{act}, when $\Gamma_{\mathrm{act}} = \Gamma_{\mathrm{opt}}$ in a multi-element array. To have $\Gamma_{\mathrm{act}} = \Gamma_{\mathrm{opt}}$ irrespective of the beamformer coefficients, the array antennas should be fully decoupled. In practical arrays, mutual coupling exists, which results in $b_{\mathrm{n},1}$ to $b_{\mathrm{n,m}}$ coupling to all antennas in an array and propagating to the system output via multiple paths thereby making the total output power beamformer dependent, and the required destructive interference of $\mathbf{a}_{\mathrm{n}}$ with $\mathbf{b}_{\mathrm{n}}$ is beamformer specific and influences Γ_{act}.

As noise waves $b_{\mathrm{n},1}$ to $b_{\mathrm{n,m}}$ propagate among the m elements of the array, they experience delays τ_{delay} that consist of the following: $\tau_{i,j}$, where $i, j = 1 \ldots m$ and $i \neq j$, due to the physical distance between antenna elements; τ_{d} due to the length of the antenna-feed network; and τ_{tx} due to any transmission lines that may be used between antenna output ports and the receiver inputs. When delayed, $\mathbf{b}_{\mathrm{n}}$ correlation with $\mathbf{a}_{\mathrm{n}}$ becomes dependent on the receiver bandwidth, f_{B}. Intuitively then, one would expect that the combination of the receiver bandwidth and delays should increase T_{rec}, since destructive interference requires correlation. It is also expected that in this case Γ_{act} should move closer to the center of the Smith chart, since $\Gamma_{\mathrm{act}} = 0$ is optimum when $\mathbf{b}_{\mathrm{n}}$ and $\mathbf{a}_{\mathrm{n}}$ are uncorrelated.

An m-element antenna array S-parameter matrix, $\mathbf{S}_{\mathrm{A}} \in \mathbb{C}^{m\times m}$, consists of complex elements for each measured frequency that are determined over a bandwidth $f_{B0} = 1$ Hz, thereby representing the effects of delays experienced by signals by their associated phases. The effect of the delays, τ_{delay}, on $\mathbf{S}_A$ at each operating frequency can be represented by the Fourier transforms of delay terms as

$$\mathbf{S}_A = \begin{bmatrix} S_{11}e^{-j\omega(2\tau_d+2\tau_{tx})} & \cdots & S_{1m}e^{-j\omega(2\tau_d+\tau_{1m}+2\tau_{tx})} \\ \vdots & \ddots & \vdots \\ S_{m1}e^{-j\omega(2\tau_d+\tau_{m1}+2\tau_{tx})} & \cdots & S_{mm}e^{-j\omega(2\tau_d+2\tau_{tx})} \end{bmatrix}. \quad (3)$$

We next represent $\mathbf{R}_{rec}$ in terms of travelling-wave NPs [21, p. 54] $\mathbf{T}_\alpha = E\{\mathbf{a}_n\mathbf{a}_n^\dagger\}/2k_b f_{B0}$, $\mathbf{T}_\beta = E\{\mathbf{b}_n\mathbf{b}_n^\dagger\}/2k_b f_{B0}$, and $\mathbf{T}_\gamma = E\{\mathbf{b}_n\mathbf{a}_n^\dagger\}/2k_b f_{B0}$, where $E\{\cdot\}$ denotes expectation, as [14]

$$\mathbf{R}_{rec} = 2k_b f_{B0}\left(\mathbf{T}_\alpha + \mathbf{S}_A\mathbf{T}_\beta\mathbf{S}_A^\dagger - \mathbf{S}_A\mathbf{T}_\gamma - \mathbf{T}_\gamma^\dagger\mathbf{S}_A^\dagger\right). \quad (4)$$

To determine T_{rec} for a receiver operating over a bandwidth f_B, the numerator and the denominator of (1) are integrated over $f_B = f_H - f_L$ to obtain

$$T_{rec} = \frac{\mathbf{w}^\dagger\left[\int_{f_L}^{f_H}\mathbf{G}\left(\mathbf{T}_\alpha + \mathbf{S}_A\mathbf{T}_\beta\mathbf{S}_A^\dagger - 2\Re\{\mathbf{S}_A\mathbf{T}_\gamma\}\right)\mathbf{G}^\dagger \mathrm{d}f\right]\mathbf{w}}{\mathbf{w}^\dagger\left[\int_{f_L}^{f_H}\mathbf{G}\left(\mathbf{I} - \mathbf{S}_A\mathbf{S}_A^\dagger\right)\mathbf{G}^\dagger \mathrm{d}f\right]\mathbf{w}}, \quad (5)$$

where in general each term under the integrals is frequency dependent, and Bosma's theorem [19] was used to expand $\mathbf{R}_t$ in terms of $\mathbf{S}_A$. It is important to highlight here that prior works assumed that over f_B all terms are independent of frequency and ignored decorrelation between $\mathbf{b}_n$ and $\mathbf{a}_n$ thus simply leading to (1).

While previous works [12, 15] have demonstrated that for each LNA $\#i$ $(1 \le i \le m)$ there is a unique Γ_{act}, found from

$$\Gamma_{act,i} = \frac{1}{w_{f,i}^*}\sum_{j=1}^{m} w_{f,j}^* S_{A,ji}, \quad (6)$$

where $w_{f,j}^*$ are conjugated elements of $\mathbf{w}_f \equiv \mathbf{G}^\dagger\mathbf{w}$ [15], to limit the number of m different LNA designs, in practice all LNAs are designed the same. Therefore, this work also assumes identical LNAs. We then identify the optimum Γ_{opt}, denoted as Γ_{act}, of the LNA that minimizes T_{rec} in (5) for a given set of beamformer coefficients $\mathbf{w}$.

To do this, we first express travelling-wave NPs in terms of conventional NPs, T_{min} (minimum noise temperature), $Y_{opt} = G_{opt} + jB_{opt}$ (the optimum admittance for minimum noise), and N (Lange invariant), to obtain [21]

$$\begin{cases} T_\alpha = T_{min} + T_0\frac{N}{G_{opt}R_0}\left|1 - R_0Y_{opt}\right|^2, \\ T_\beta = -T_{min} + T_0\frac{N}{G_{opt}R_0}\left|1 + R_0Y_{opt}\right|^2, \\ T_\gamma = T_0\frac{N}{G_{opt}R_0}\left(1 + R_0Y_{opt}\right)\left(1 - R_0Y_{opt}^*\right), \end{cases} \quad (7)$$

where N is preferred over another NP $R_n \equiv N/G_{opt}$ (the noise equivalent resistance) due to its invariance under lossless transformations. Then, in contrast to prior works of assuming m different LNAs [14], to minimize T_{rec}, we find one optimum $Y_{opt} = R_0^{-1}(1 - \Gamma_{opt})/(1 + \Gamma_{opt})$, denoted as $Y_{act} \equiv R_0^{-1}(1 - \Gamma_{act})/(1 + \Gamma_{act})$, that minimizes T_{rec} via $\partial T_{rec}/\partial Y_{opt} = 0$ by first solving for B_{act} from $\partial T_{rec}/\partial B_{opt} = 0$ and then for G_{act} from $\partial T_{rec}/\partial G_{opt} = 0$ to obtain

$$B_{act} = \frac{-2\mathbf{w}^\dagger\left[\int_{f_L}^{f_H}\mathbf{G}\Im\{\mathbf{S}_A\}\mathbf{G}^\dagger \mathrm{d}f\right]\mathbf{w}}{R_0\mathbf{w}^\dagger\left[\int_{f_L}^{f_H}\mathbf{G}\left[\mathbf{I} + \mathbf{S}_A\mathbf{S}_A^\dagger + 2\Re\{\mathbf{S}_A\}\right]\mathbf{G}^\dagger \mathrm{d}f\right]\mathbf{w}}, \quad (8)$$

$$G_{act}^2 = \frac{\mathbf{w}^\dagger\left[\int_{f_L}^{f_H}\mathbf{G}\left[\left(1 + R_0^2B_{act}^2\right)\left(\mathbf{I} + \mathbf{S}_A\mathbf{S}_A^\dagger\right)\right)\right)}{R_0^2\mathbf{w}^\dagger\left[\int_{f_L}^{f_H}\mathbf{G}\left[\mathbf{I} + \mathbf{S}_A\mathbf{S}_A^\dagger + 2\Re\{\mathbf{S}_A\}\right]\mathbf{G}^\dagger \mathrm{d}f\right]\mathbf{w}} \quad (9)$$

$$-\frac{\left((2\Re\left\{\left(1 + j2R_0B_{act} - R_0^2B_{act}^2\right)\mathbf{S}_A\right\}\right]\mathbf{G}^\dagger \mathrm{d}f\right]\mathbf{w}}{R_0^2\mathbf{w}^\dagger\left[\int_{f_L}^{f_H}\mathbf{G}\left[\mathbf{I} + \mathbf{S}_A\mathbf{S}_A^\dagger + 2\Re\{\mathbf{S}_A\}\right]\mathbf{G}^\dagger \mathrm{d}f\right]\mathbf{w}}. \quad (9)$$

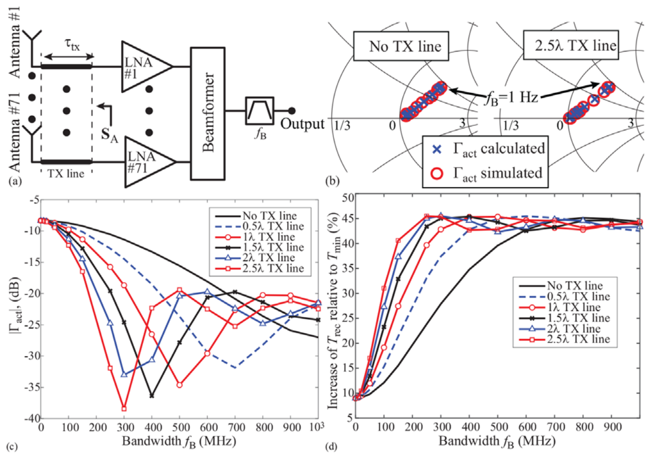

Fig. 2 *Simulated Γ_{act} and T_{rec} as a function of f_B of a 71-element Vivaldi antenna array operating at 1.4 GHz: (a) Block diagram with TX lines; (b) Γ_{act} as function of f_B; (c) Γ_{act} [dB] as function of f_B; and (d) T_{rec} as function of f_B*

Since real and imaginary parts of Y_{act} in (9) and (8) are functions of delays through $\mathbf{S}_A$ and bandwidth through the integration, the anticipated dependence of Γ_{act} on the receiver bandwidth is identified. In addition to the bandwidth-dependent decorrelation of $\mathbf{a}_n$ and $\mathbf{b}_n$, the expressions in (5), (8), and (9) also allow us to incorporate frequency variations of $\mathbf{S}_A$, $\mathbf{G}$, and NPs that naturally exist in practice and to analyze the effect of bandwidth on T_{rec} and Γ_{act}.

Simulation results with a 71-element array: We next illustrate the dependence of Γ_{act} and T_{rec} on bandwidth f_B using simulations. The simulations were simplified by setting the LNA NPs and the magnitude of $\mathbf{S}_A$ constant over bandwidth. This simplification was made intentionally to focus strictly on the effects of $\mathbf{a}_n$ and $\mathbf{b}_n$ decorrelation on Γ_{act} and T_{rec}, which is the unique focus of this work. However, the LNA NPs and $\mathbf{S}_A$ frequency dependence can be readily accommodated by accounting for them in $\mathbf{T}_\alpha$, $\mathbf{T}_\beta$, $\mathbf{T}_\gamma$, $\mathbf{S}_A$, and $\mathbf{G}$ under integrals in (5), (8), and (9). This additional frequency dependence would further exacerbate the impact f_B on T_{rec} and Γ_{act}, but would obscure the intended demonstration of the noise decorrelation impact.

In these simulations, a 1.4-GHz EM model of a 71-element dual-polarized Vivaldi focal-plane array for a Square Kilometer Array demonstrator was taken from [22]. Since each polarization has its own beamforming network, the beamformer coefficients associated with the 36 vertically polarized antennas were assigned unity value whereas the 35 coefficients associated with horizontal polarized antennas were set to zero. We introduced delays to the S-parameters by first calculating physical distances between each antenna element and the length of each antenna and then assuming that signals propagate across antennas at approximately the speed of light to calculate the delays. These delays are approximate but sufficient to demonstrate the dependence of Γ_{act} and T_{rec} on f_B. Once delays were found, we adjusted the phases of the S-parameters by the phase associated with the calculated delays at 1.4 GHz. By doing so, the combined phase of each element of $\mathbf{S}_A$ at 1.4 GHz remains unaltered.

The receiver was implemented with LNAs from [23] having $T_{min} = 15$ K and $N = 0.024$. Note that in this and the previous sections, we make use of noise parameter N [24], which, like T_{min}, is invariant under lossless transformations and is independent of Γ_{opt}. Therefore, the search for Γ_{act} can proceed by setting LNA Γ_{opt} to each value in a set of 18141 values spread over an entire Smith chart and monitoring T_{rec} until minimum T_{rec} is identified. This process of modifying Γ_{opt} is equivalent to employing a lossless matching network between the antenna array and LNAs. The block diagram of the simulated system is shown in Figure 2a, where TX line represents some length of transmission lines, if any, connecting the receiver LNAs to the array. In our simulations, we have used TX lines that are multiple of half of the wavelength, λ, at 1.4 GHz. Such transmission lines do not affect the array S-parameters at the band center but they do introduce delays experienced by noise waves travelling through the network. These delays exacerbate the effect of f_B on T_{rec} and Γ_{act} even though the S-parameters at 1.4 GHz are identical for all such transmission lines.

Once Γ_{act} is found with simulations, it is compared to Γ_{act} found via Y_{act} from (8) and (9). Figure 2b, demonstrates the results for two different TX lines. As shown, Γ_{act} follow the same trajectory in both cases, but for the longer TX line the rate of change in Γ_{act} position is more rapid as can be deduced from Figure 2c that shows another representation of the results in Figure 2b and for four other TX lines. As expected, the starting points, when $f_B = 1$ Hz, are the same regardless of TX lines, but longer TX lines accelerate the change of Γ_{act} with f_B.

Figure 2d shows the impact of f_B on T_{rec}. For the array, T_{rec} is 9% higher than the LNA T_{min} when $f_B = 1$ Hz, mainly due to array noise-matching efficiency [15]. However, $f_B = 200$ MHz results in ˜20% increase even when no TX lines between the array and the LNA are inserted. Figure 2d also shows that for a 1λ TX line, there is nearly 20% increase in T_{rec} over T_{min} for $f_B = 100$ MHz. This increases to ˜31% for a 2.5λ transmission line. It is also observed that for lower f_B, the impact of the TX-line lengths on increase in T_{rec} is proportional to $f_B \times \tau_{delay}$ as expected [17] until $\mathbf{a}_n$ and $\mathbf{b}_n$ become uncorrelated, and T_{rec} comes near its maximum. The delay-bandwidth product $f_B \times \tau_{delay}$ is therefore seen as a convenient estimate to the severity of the noise decorrelation problem when scaling systems to wider bandwidths.

Discussion and conclusions: The impact of noise bandwidth on array Γ_{act} and T_{rec} is investigated. It is shown that as bandwidth increases, T_{rec} increases to as much as 45.5% of LNA T_{min} for the 71-element array used in this work. While the increase in T_{rec} may be insignificant for some applications that operate over a modest noise bandwidth, for ultra-wideband systems, such as a WiGig radio ($f_B = 2$ GHz), DARPA's WARP radios ($f_B = 16$ GHz), and ultra-sensitive military AESA radars, full decorrelation of LNA noise waves is very possible, particularly if even short TX lines in an order of 1 cm are used to connect antenna arrays to receivers, resulting in increase of T_{rec} much higher than would be calculated using prior methods.

Acknowledgement: The authors would like to thank Dr. Bruce Veidt from NRC Herzberg for providing S-parameters of the array from [22].

Received: *16 November 2020* Accepted: *16 November 2020*
doi: 10.1049/ell2.12018

References

1 de Zwart, J.A., et al.: Design of a SENSE-optimized high-sensitivity MRI receive coil for brain imaging. *Magn. Reson. Med.* **47**(6), 1218–1227 (2002)

2 Krieger, G., Gebert, N., Moreira, A.: Multidimensional waveform encoding: A new digital beamforming technique for synthetic aperture radar remote sensing. *IEEE Trans. Geosci. Remote Sens.* **46**(1), 31–46 (2008)

3 Heath, T., et al.: Simultaneous, multi-frequency synchronous oscillator antenna. In: *IEEE Military Communications Conference*, pp. 1–7, San Diego (2008)

4 Dewdney, P., et al.: The Square Kilometre Array. *Proc. IEEE* **97**(8), 1482–1496 (2009)

5 Zhang, R., et al.: Multi-antenna based spectrum sensing for cognitive radios: A GLRT approach. *IEEE Trans. Commun.* **58**(1), 84–88 (2010)

6 Brookner, E.: Never ending saga of phased array breakthroughs. In: *IEEE International Symposium on Phased Array Systems and Technology (ARRAY)*, pp. 61–73, Waltham (2010)

7 Heo, D., Warnick, K.F.: Integrated eight element Ku band transmit/receive beamformer chipset for low-cost commercial phased array antennas. In: *IEEE International Symposium on Phased Array Systems and Technology (ARRAY)*, pp. 653–659, Waltham (2010)

8 Natarajan, A., et al.: A fully-integrated 16-element phased-array receiver in SiGe BiCMOS for 60-GHz communications. *IEEE Journal of Solid-State Circuits* **46**(5), 1059–1075 (2011)

9 Inac, O., et al.: A 90-100-GHz phased-array transmit/receive silicon RFIC module with built-in self-test. *IEEE Trans. Microwave Theory Tech.* **61**(10), 3774–3782 (2013)

10 Rappaport, T.S., et al.: Wireless communications and applications above 100 GHz: Opportunities and challenges for 6G and beyond. *IEEE Access* **7**, 78 729–78 757 (2019)

11 Rajatheva, N., et al.: White paper on broadband connectivity in 6G. [Online]. https://arxiv.org/pdf/2004.14247.pdf, (Accessed: August 8, 2020).

12 Maaskant, R., Woestenburg, E.: Applying the active antenna impedance to achieve noise match in receiving array antennas. In: *IEEE Antennas and Propagation International Symposium*, pp. 5889–5892, Honolulu (2007)

13 Ivashina, M.V., Maaskant, R., Woestenburg, B.: Equivalent system representation to model the beam sensitivity of receiving antenna arrays. *IEEE Antennas Wirel. Propag. Lett.* **7**, 733–737 (2008)

14 Warnick, K., et al.: Minimizing the noise penalty due to mutual coupling for a receiving array. *IEEE Trans. Antennas Propag.* **57**(6), 1634–1644 (2009)

15 Warnick, K.F., et al.: Unified definitions of efficiencies and system noise temperature for receiving antenna arrays. *IEEE Trans. Antennas Propag.* **58**(6), 2121–2125 (2010)

16 Belostotski, L., et al.: Low noise amplifier design considerations for use in antenna arrays. *IEEE Trans. Antennas Propag.* **63**(6), 2508–2520 (2015)

17 Sheldon, A., et al.: Impact of noise bandwidth on noise figure. *IEEE Trans. Instrum. Meas.* **68**(7), 2662–2664 (2019)

18 Thompson, A.R., Moran, J.M., Swenson Jr., G.W.: *Interferometry and Synthesis in Radio Astronomy*. John Wiley & Sons, New York (1986)

19 Bosma, H.: On the theory of linear noisy systems. *Philips Res. Rep., Supplement* (10), 1–189 (1967)

20 Belostotski, L.: No noise is good noise: Noise matching, noise canceling, and maybe a bit of both for wide-band LNAs. *IEEE Microwave Mag.* **17**(8), 28–40 (2016)

21 Engberg, J., Larsen, T.: *Noise Theory of Linear and Nonlienar Circuits*. John Wiley & Sons, West Sussex, UK (1995)

22 Sarkis, R., Veidt, B., Craeye, C.: Fast numerical method for focal plane array simulation of 3D Vivaldi antennas. In: *International Conference on Electromagnetics in Advanced Applications*, pp. 772–775, Torino, Italy (2012)

23 Beaulieu, A.J., et al.: Noise performance of a phased-array feed with CMOS low-noise amplifiers. *IEEE Antennas Wirel. Propag. Lett.* **15**, 1719–1722 (2016)

24 Belostotski, L.: On the number of noise parameters for analyses of circuits with MOSFETs. *IEEE Trans. Microwave Theory Tech.* **59**(4), 877–881 (2011)